



## Hydrogen evolution and permeation into steel during zinc electroplating; effect of organic additives

L. MIRKOVA<sup>1\*</sup>, G. MAURIN<sup>2</sup>, I. KRASDEV<sup>1</sup> and C. TSVETKOVA<sup>1</sup>

<sup>1</sup>Institute of Physical Chemistry, Bulgarian Academy of Sciences, Department "Elchim", Acad. G. Bonchev, bl. 11, 1113 Sofia, Bulgaria

<sup>2</sup>UPR 15 du CNRS "Physique des Liquides et Electrochimie", Tour 22, 4 place Jussieu, 75252 Paris cedex 05, France  
(\*author for correspondence, e-mail: mirkova@ipchp.ipc.bas.bg)

Received 11 July 2000; accepted in revised form 21 November 2000

**Key words:** additives, hydrogen permeation, steel substrate, zinc deposition

### Abstract

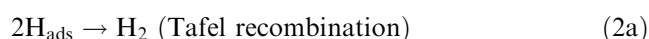
The Devanathan and Stachurski diffusion membrane method was used to study the evolution of hydrogen and its permeation into a steel sheet during cathodic charging from a chloride electrolyte or during zinc electroplating. The influence of four different organic compounds, which are the components of various formulations derived to improve zinc electrocoatings, were also tested. At a high-charging current density, the permeation transients obtained in a chloride electrolyte without zinc ions exhibit a maximum attributed to hydrogen trapping in the subsurface layer on the entry side. The concentration of adsorbed hydrogen on the steel surface depends not only on the cathodic current density and the composition of the solution, but also on the influence of the organic additives on the recombination of hydrogen atoms. During zinc electrodeposition, the coating covers the substrate in a few seconds and acts as a barrier for hydrogen absorption. The permeation rate depends on the cathodic current density but also on the concentration of ZnCl<sub>2</sub> in correlation with the porosity of the coating. It is shown that steel substrate hydrogenation (beneath the zinc coating) is strongly reduced in the presence of a combined additive, composed of four compounds in appropriate amounts as well as in the presence of PEG<sub>6000</sub> in the plating bath. This effect, which is correlated to the modification of the hydrogen evolution process, can be used to hinder the severe drawbacks caused by hydrogen penetration into the steel substrate.

### 1. Introduction

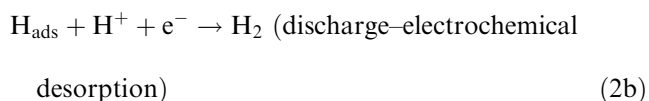
Zinc and its alloys are widely used as sacrificial materials for corrosion protection of steel. However, zinc electrodeposition is accompanied by the simultaneous hydrogen evolution reaction (HER) which affects the current efficiency, especially in alkaline medium. The HER mechanism on iron and steel in various solutions has been widely studied [1–5]. It has been found by Devanathan and Stachurski [5] that the HER mechanism on iron in acidic medium is rate-determining discharge, followed by Tafel recombination at low overpotential, or by electrochemical desorption at high overpotential. The mechanism of HER can be presented simply by the following scheme:



The major part of adsorbed hydrogen reacts to give hydrogen molecules evolving to atmosphere:



or



At the same time, a fraction may diffuse into the steel substrate



The HER mechanism and hydrogen absorption has been discussed in detail [6, 7], and recent reviews on this topic have been presented [8, 9].

Absorbed hydrogen may cause severe detrimental effects on the mechanical properties of steel, such as reduction in ductility, formation of blisters, and loss of mechanical strength leading to hydrogen embrittlement [10]. These phenomena have been attributed to an effect of internal pressure, adsorption, decohesion of the grains, or to the formation of hydride [11]. During zinc electroplating on steel, hydrogen evolution and permeation occurs mainly in the initial stages, when the steel

surface is not totally coated [12, 13]. It has been also suggested that hydrogen is trapped in the deposit before diffusing into the substrate [14].

Most work, reported on hydrogen permeation in thin iron or steel foil during cathodic charging were performed under galvanostatic or potentiostatic conditions using the electrochemical technique derived by Devanathan and Stachurski [5, 15, 16]. The presence of a maximum in the permeation transients obtained in 0.2 M  $\text{H}_2\text{SO}_4$ , as well as the apparent decrease in substrate permeability at high current densities was reported [17–22] and was attributed to the onset of hydrogen embrittlement [18]. Beck et al. [19] explained this maximum by the formation of pores or blisters in the metal in which the hydrogen was trapped during diffusion or by the formation of surface cracks due to supersaturation of the metal with hydrogen. Thus, when the concentration of hydrogen in the metal exceeds its saturation value, corresponding to a critical cathodic current density, the hydrogen atoms diffuse to the surface of small crevices and voids in the metal and recombine there to form  $\text{H}_2$ , which can generate a high internal pressure, expand the crevices and voids, and cause further cracking. It is suggested, that nucleation sites for blisters and cracks which lead to embrittlement of the substrate are aggregates of dislocations. According to Wach et al. [21, 22], the maximum hydrogen permeation rate,  $I_p$ , may be attributed to the formation of an effective barrier, or series of barriers, of adsorbed surface hydrogen. The internal part of the barrier may be due to a high local hydrogen concentration able to impede the penetration of hydrogen into the metal. It is suggested that the barrier could be accepted as a very thin layer of the  $\beta$ -phase, reported in [10] or that it is merely hydrogen saturated layer. This layer decays with time on interruption of the polarizing current, and the decay can be accelerated by the application of an alternating current or anodic polarization at very low current densities [21]. As reported by Amrani et al. [23], electrolytic hydrogen does not permeate in iron membranes at a constant rate. The permeation flux fluctuates with the evolution of hydrogen bubbles at the electrode; under attached bubbles the decrease of adsorbed hydrogen concentration limits the hydrogen absorption. After bubble evolution, adsorption and absorption rates increase.

The Devanathan and Stachurski technique was also widely used to detect hydrogen permeation occurring during electroplating [13, 14, 16, 24, 25]. It was observed that the permeation rate can be strongly influenced by addition of organic compounds to the electrolyte. For example, in previous work related to zinc electrodeposition from an alkaline bath, it was observed that steel hydrogenation is enhanced by Na-benzylnicotinate, while it is inhibited by anisaldehyde bisulphite [13]. The mechanism of action of additives is still a topic of dispute. According to [26], the additives, by a blocking reaction (Reaction 2), increase the amount of adsorbed hydrogen and, as a result, the rate of hydrogen

absorption (Reaction 3). These additives are hydrogen embrittlement promoters. On the other hand, additives which slow down the formation of atomic hydrogen (Reaction 1), would act as embrittlement reducers. Usually, additives prepared to improve the quality of zinc electrocoatings are a combination of organic compounds, such as a mixture of polyalcohol with a high molecular weight (MW), surface-active agent (SAA), brightener and other appropriate chemicals.

In this work, voltammetry and the Devanathan and Stachurski diffusion membrane technique were used to study the evolution of hydrogen and its permeation into the steel substrate during cathodic charging from a medium acidic chloride solution or during zinc electroplating. Particular attention was paid to the effects of four different organic compounds representing components of a formulation [27] which was previously derived to improve zinc coating quality.

## 2. Experimental details

The zinc plating bath was prepared by adding 0.12 to 0.72 M  $\text{ZnCl}_2$  and 0.24 M  $\text{H}_3\text{BO}_3$  in a 2.7 M KCl aqueous solution (room temperature, adjusted pH 4.0). A blank solution containing only 2.7 M KCl and 0.24 M  $\text{H}_3\text{BO}_3$  was also used. All reagents were of analytical grade. The following four organic compounds were also tested: Na-benzoate (Na-B), 6 g  $\text{l}^{-1}$ ; polyethyleneglycol (PEG) with MW = 6000, 6 g  $\text{l}^{-1}$ ; surface active agent (SAA): ethoxylated aliphatic alcohol, 2 g  $\text{l}^{-1}$ ; and benzalacetone (BA), 0.5 g  $\text{l}^{-1}$ .

The required concentration of Na-B, PEG and SAA in the electrolyte was obtained by adding the appropriate amount of their aqueous solution, whereas the required concentration of BA was obtained by adding the appropriate amount of its methanol solution.

Experiments were carried out in a Devanathan and Stachurski set up made of two symmetrical electrochemical cells mounted on both sides of the horizontal steel membrane. The upper cell (polarization cell) was used to evolve hydrogen in the blank electrolyte or to deposit zinc from the plating bath. The lower cell (ionization cell) was used to oxidize hydrogen which diffused through the metal foil. The ionization current, registered under potentiostatic control vs a Hg/HgO reference electrode at the exit side of the membrane is a direct measure of the hydrogen permeation rate  $I_p$ . Both cells were equipped with a platinum grid as counter electrodes.

The steel membranes were prepared from a 100  $\mu\text{m}$  thick unannealed cold-rolled sheet of mild steel (Willy Traub, GmbH & Co.). Before experiments, membranes were degreased in acetone, rinsed, ultrasonically cleaned in ethanol and etched in 1/1 HCl solution. The exit side was plated with a thin palladium layer. After Pd plating, the membranes were cathodically degreased for 30 s, rinsed and mounted between the cells. The exposed area was 2  $\text{cm}^2$ . A 0.5 M NaOH solution was introduced into

the ionization cell and a  $-150$  mV (Hg/HgO) potential was applied to reduce surface oxides. Then the potential was established to  $+150$  mV. When the anodic current density reached a low steady value (typically below  $1.5 \mu\text{A cm}^{-2}$ ) the electrolyte, deoxygenated by a gentle argon bubbling, was introduced in the polarization cell and a constant cathodic current density  $I_c$  was applied on the upper face of the membrane thanks to a galvanostat. The permeation current was recorded against time until reaching a steady-state.

Linear sweep voltammetry and chronopotentiometry were also used to obtain additional data for zinc deposition mechanism. The voltammograms and current–time transients were obtained by using an electrochemical system (Princeton Applied Research, model 263 A). The three-electrode cell was supplied with a steel working electrode (surface area  $1 \text{ cm}^2$ ), a Pt counter electrode and Ag/AgCl reference electrode. The potential sweep was performed in the cathodic range from  $-0.5$  to  $-1.6$  to  $-0.5$  V vs Ag/AgCl with a scan rate of  $25 \text{ mV s}^{-1}$ . The current–time transients were obtained at a potential step from  $-0.4$  to  $-1.3$  V vs Ag/AgCl during 10 s.

### 3. Results and discussion

#### 3.1. Hydrogen permeation from the blank electrolyte

In a preliminary study, experiments were performed using the blank electrolyte where only hydrogen was discharged and evolved on the cathode surface at constant current densities between  $10$  and  $80 \text{ mA cm}^{-2}$ . Permeation  $I_p$  against  $t$  responses are presented on Figure 1. In all cases, at the beginning of the permeation experiments, it was observed that  $I_p$  was negligible during a time delay  $t_d$ . The duration of  $t_d$  was between  $0.5$  and  $2$  min and decreased with increase in cathodic current density. The origin of this delay will be discussed in a further paper. An increase in  $I_c$  induced an increase

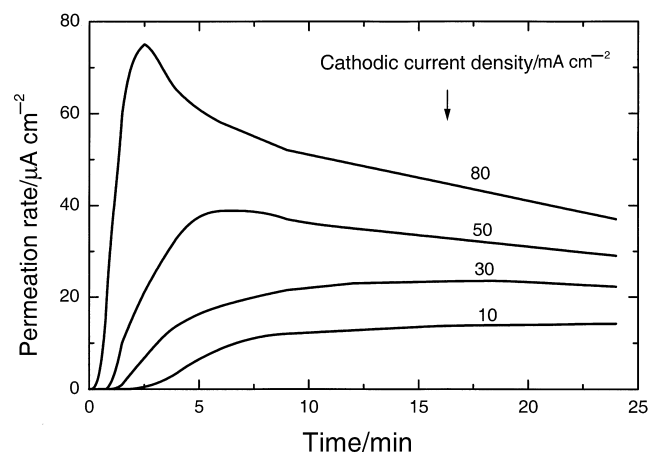


Fig. 1. Hydrogen permeation transients obtained in the 2.7 M KCl blank electrolyte at various cathodic current densities. CD: (a) 80, (b) 50, (c) 30 and (d) 10  $\text{mA cm}^{-2}$ .

in the hydrogen permeation rate. However, the shape of the permeation transients varied with the charging current density. For  $I_c < 30 \text{ mA cm}^{-2}$ , the transients exhibit a normal diffusion behaviour:  $I_p$  tended monotonously to a steady-state value ( $I_p^{st}$ ). For higher values of  $I_c$  the permeation curves became more complex: within few minutes  $I_p$  passed through a maximum ( $I_p^{max}$ ) and then decayed to a steady-state value. For  $I_c = 80 \text{ mA cm}^{-2}$ , the increase in  $I_p$  was very sharp (within 2.5 min) and a clear maximum was observed.

The rise of  $I_p$  with  $I_c$  can be ascribed to the larger coverage ( $\theta_H$ ) of the surface with the adsorbed hydrogen atoms ( $H_{ads}$ ) and/or to a higher rate of Reaction 3, producing absorbed hydrogen atoms ( $H_{abs}$ ) in the subsurface layer of the steel. The permeation efficiency, expressed by the ratio  $I_p/I_c$  and calculated after 10 or 25 min from the beginning of the process is presented on Table 1. It can be observed that permeation tends to decrease with time at  $50$  and  $80 \text{ mA cm}^{-2}$  and that the permeation efficiency decreases with increasing cathodic current density both at 10 min and at 25 min. Hence, it appears that the membrane becomes more impermeable when hydrogen is evolved at a high rate on the input side of the membrane.

The presence of a maximum in the permeation transients, as well as the apparent decrease in the substrate permeability at high current densities, are not expected from common theoretical considerations. However, as described above, similar behaviour was observed and attributed to the onset of hydrogen embrittlement. Such a maximum was explained by the formation of pores or blisters within the metal in which the hydrogen was trapped during diffusion, or by the formation of surface cracks due to supersaturation of the metal with hydrogen when a critical cathodic current density was reached.

To verify these assumptions, additional experiments were carried out with the blank solution at  $80 \text{ mA cm}^{-2}$ , either by mechanically stirring the solution in the upper cell or by adding  $2 \text{ mg l}^{-1}$  of sodium-dodecyl sulphate, a surfactant which facilitates the departure of hydrogen bubbles and which is known as an ‘antipitting’ agent. In both cases, the maximum in the  $I_p$  against  $t$  curves was suppressed (Figure 2) and, moreover, a slower increase in permeation rate with time was observed. It can be concluded that the acceleration of the departure of hydrogen, either by a hydrodynamic effect or by the

Table 1. Values of the hydrogen permeation current density  $I_p$  and hydrogen permeation efficiency  $I_p/I_c$  after 10 or 25 min for various cathodic current densities  $I_c$  in a blank 2.7 M KCl solution

$I_c/\text{mA cm}^{-2}$	$I_p/\mu\text{A cm}^{-2}$		$I_p/I_c/\%$	
	10 min	25 min	10 min	25 min
10	12.25	14.2	0.123	0.142
30	22	22	0.073	0.073
50	36	28	0.072	0.056
80	51	36	0.064	0.045

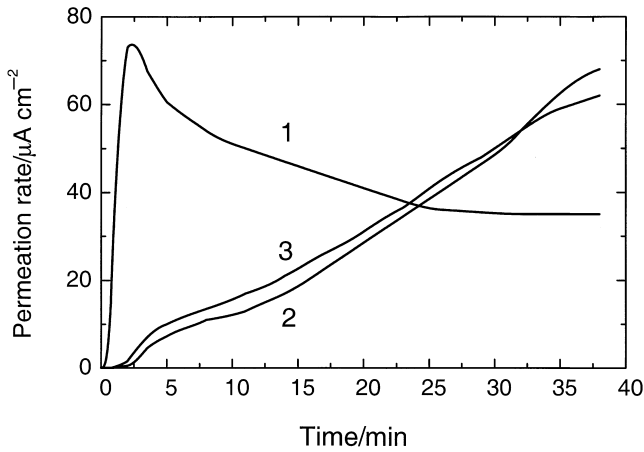


Fig. 2. Hydrogen permeation transients obtained in the 2.7 M KCl blank electrolyte at  $80 \text{ mA cm}^{-2}$ : (1) steady electrolyte without a surfactant; (2) in the presence of a surfactant; and (3) stirred electrolyte.

decrease of the wetting forces by the surfactant, contributed to lowering the barrier of adsorbed hydrogen as proposed by Wach et al. [21, 22].

Figure 3 shows a plot of  $I_p^{\text{st}}$  against the square root of recombination current  $I_r$  where  $I_r = I_c - I_p^{\text{st}}$ . A satisfactory straight line passes through the origin and confirms that HER proceeds via the Tafel recombination (Reaction 2(a)) [6, 28].

In the steady state,  $I_p^{\text{st}}$  is related to the concentration  $C_0$  ( $\text{mol cm}^{-3}$ ) of hydrogen atoms just under the cathodic surface at the input side of the membrane by Equation 4 [20, 29]:

$$I_p^{\text{st}} = FDC_0/L \quad (4)$$

where  $F$  is the faradaic constant,  $D$  the hydrogen diffusion coefficient in the metal, and  $L$  the thickness of the membrane. Equation 4 reveals that any alteration of the steady-state permeation rate results from an alteration of  $C_0$  (at a constant  $D$  and  $L$ ).

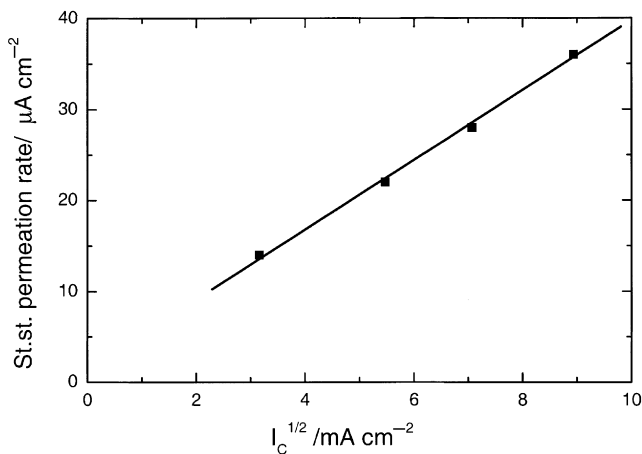


Fig. 3. Steady state permeation current density vs square root of the cathodic current density (blank electrolyte).

To evaluate  $D$  ( $\text{cm}^2 \text{ s}^{-1}$ ) from the permeation transient, Equation 5 was proposed [20, 29]:

$$D = \frac{0.138 L^2}{t} \quad (5)$$

where  $t$  is the time required for  $I_p$  to reach half of its steady-state value.

The diffusion coefficient  $D$  was calculated from the first transient, obtained at the lower experimental polarization current density ( $I_c = 10 \text{ mA cm}^{-2}$ ), because only this transient has the expected monotonic shape. The calculated value of  $D$  was  $0.4 \times 10^{-7} \text{ cm}^2 \text{ s}^{-1}$  which is in satisfactory agreement with the data reported in [16]. The calculated values of  $C_0$  assuming that  $D$  is constant are reported on Table 2 as a function of  $I_c$ .

From these data it appears that the increase in hydrogen permeation is correlated to that of the hydrogen concentration just under the input face caused by the increasing cathodic current density, that is, either by an increase in  $\theta_H$  or by a shift in the equilibrium position of the reaction  $\text{H}_{\text{ads}} \rightleftharpoons \text{H}_{\text{abs}}$  toward  $\text{H}_{\text{abs}}$ .

The influence of Na-B, PEG, SAA and BA addition to the blank solution on HER and on hydrogen permeation were studied by recording polarization curves (Figure 4) and permeation transients (Figure 5), respectively. As seen on Figure 4, the presence of Na-B or PEG induced a significant increase in the hydrogen evolution rate at potentials more negative than  $-1.40 \text{ V}$ ; the chosen value of electrodeposition current density

Table 2. Steady state permeation rate  $I_p^{\text{st}}$  and hydrogen concentration  $C_0$  at the input surface of steel during polarization for various cathodic current densities in a blank 2.7 M KCl solution

$I_c/\text{mA cm}^{-2}$	$I_p^{\text{st}}/\mu\text{A cm}^{-2}$	$10^5 C_0/\text{mol cm}^{-3}$
10	14.2	1.9
30	22	2.9
50	28	3.6
80	36	4.7

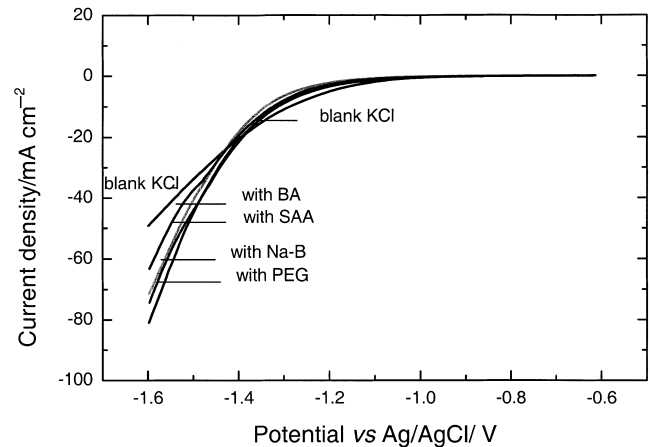


Fig. 4. Polarization curves for hydrogen evolution in the blank electrolyte without or with Na-B, PEG<sub>6000</sub>, SAA and BA additives. (Scan rate  $25 \text{ mV cm}^{-1}$ ).

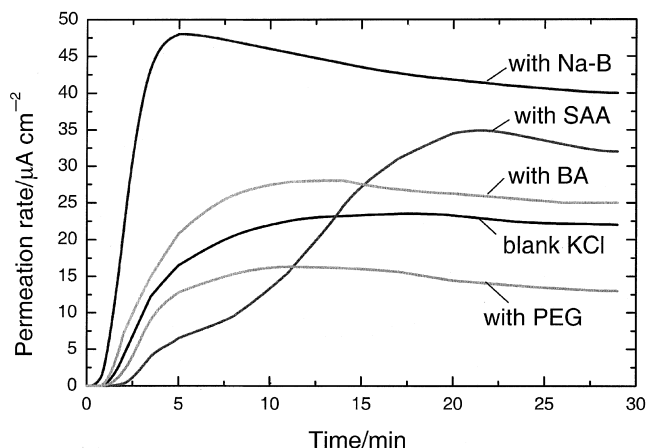


Fig. 5. Hydrogen permeation transients obtained in the blank electrolyte without or with Na-B, PEG<sub>6000</sub>, SAA and BA additives. (Charging current density 30 mA cm<sup>-2</sup>).

was 30 mA cm<sup>-2</sup> for the permeation experiments. Thus these additives can be considered as HER promoters.

From the permeation transients (Figure 5) it appears that PEG is an efficient inhibitor of hydrogenation of the steel membrane. This is in apparent contradiction with the fact that, according to Figure 4, PEG tends to increase the HER rate. It was also observed that many more hydrogen bubbles evolve in the electrolyte as compared with a blank solution. It can be assumed that this additive enhances the recombination of hydrogen atoms to form molecular hydrogen (Reaction 2) and thus decreases the surface concentration of H<sub>ads</sub>. In the presence of SAA, there is a similarity between the form of the permeation transients obtained in the presence of sodium dodecylsulphate and those of the transients obtained with mechanically stirring of the solution (see again Figure 2). Initially, this surfactant inhibited the hydrogenation process, but then the permeation rate slowly increased to a higher steady value than that of a blank solution.

In contrast, in the presence of Na-B or BA the hydrogenation process was enhanced from the beginning of polarization. In the presence of Na-B the permeation rate rose more rapidly (in less than 5 min) to a higher maximum and finally reached a larger steady value than that of a blank solution. It can be concluded that this additive strongly inhibited the recombination of hydrogen atoms (Reaction 2). As a result, the H<sub>ads</sub>

Table 3. Steady-state permeation current densities  $J_p^{st}$  and hydrogen concentration  $C_0$  at the input surface of steel during polarization at 30 mA cm<sup>-2</sup> in a 2.7 M KCl solution containing Na-B, PEG<sub>6000</sub>, SAA and BA additives

Composition	$J_p^{st}/\mu\text{A cm}^{-2}$	$10^5 C_0/\text{mol cm}^{-3}$
Blank KCl solution	22	2.9
+ Na-B	40	5.2
+ PEG <sub>6000</sub>	13	1.7
+ SAA	32	4.2
+ BA	25	3.3

coverage and, therefore,  $C_0$  were increased and the hydrogen absorption process (Reaction 3) was promoted. The  $J_p^{st}$  and  $C_0$  values corresponding to a blank electrolyte containing additives Na-B, PEG, SAA and BA are given in Table 3.  $C_0$  decreased by a factor of two in the presence of PEG, whereas it increased by a factor of two in the presence of Na-B. Thus, the various additives may change the permeation process in opposite manner depending of their effects on the recombination of adsorbed hydrogen at the steel surface.

### 3.2. Hydrogen permeation during zinc electrodeposition

During zinc electrodeposition onto steel, the steady permeation current, as defined in Equation 4, is never reached because the coating acts as a barrier for hydrogen diffusion. The permeation rate is a complex function depending both on the hydrogen evolution process and on the surface blocking by the zinc coating.

By performing potentiostatic  $I$  against  $t$  transients at a potential corresponding to zinc nucleation and growth, it was concluded that the substrate was covered by zinc within a time which depended on the applied potential, but which never exceeded few seconds.

As seen on Figures 6 and 7, hydrogen permeation during zinc deposition strongly decreased but nevertheless, it continued to occur far after complete surface covering by zinc. Thus, it can be assumed that during the first stage of zinc electrodeposition, when the substrate is still accessible to HER, a certain amount of hydrogen is charged into the subsurface layer which plays the role of a reservoir for the subsequent hydrogen permeation in the bulk of the steel. The permeation transients on Figures 6 and 7 reflects the competition between the increase in the hydrogen coverage (or permeation) with increasing current density and the increase in the blocking power of the coating due to its increased thickness.

With a low concentration of ZnCl<sub>2</sub> (0.12 M), the permeation transients (Figure 6) were similar to those

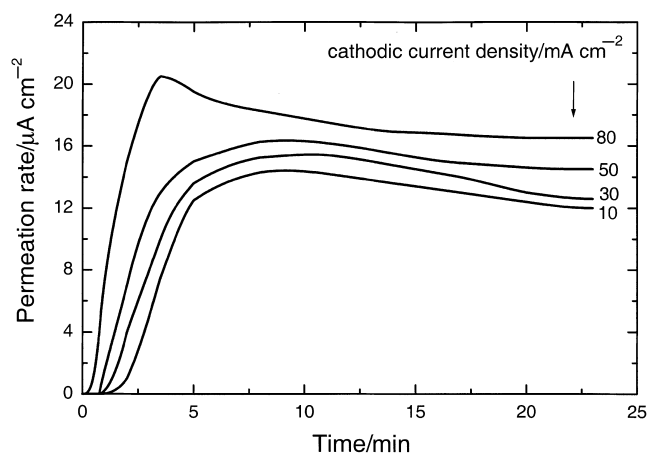


Fig. 6. Hydrogen permeation transients obtained during zinc electrodeposition at various current densities. (Zinc chloride concentration 0.12 M). CD: (a) 80, (b) 50, (c) 30 and (d) 10 mA cm<sup>-2</sup>.

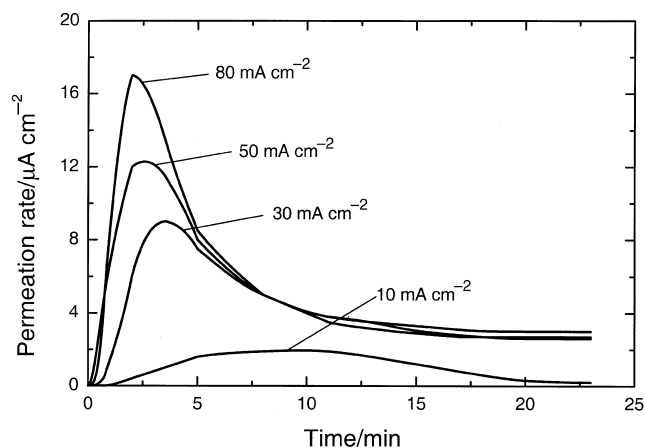


Fig. 7. Hydrogen permeation transients obtained during zinc electro-deposition at various current densities. (Zinc chloride concentration 0.24 M). CD: (a) 80, (b) 50, (c) 30 and (d) 10  $\text{mA cm}^{-2}$ .

obtained in the absence of zinc ions (Figure 1), but both the maximum and the steady-state permeation rates were decreased. The permeation rate tended to a nonzero  $I_p^{\text{st}}$  value which increased with increasing electrodeposition current density. It can be assumed that, in this case, the zinc coating, which is deposited under a partial diffusion control, is still porous and therefore, a given amount of hydrogen ions can reach the substrate. The cathodic current density determines the  $I_p^{\text{st}}$  value by controlling both the HER rate and the coating structure. According to [25], it is possible to determine the 'blocking power' of the coating and its residual porosity from the shape of the transients. Four types of transient may be expected depending on the limiting conditions. The slope of the decay curve is a direct indication of the blocking power of the coating, while the steady-state permeation rate is mainly related to the residual porosity of the coating.

For larger  $\text{ZnCl}_2$  concentrations, as seen in Figure 7 with 0.24 M  $\text{ZnCl}_2$ , the permeation rate was even more decreased and the shape of the transient curves was altered. After the maximum,  $I_p$  decayed sharply and reached a very low steady rate. In particular, for an electrodeposition current density lower than 30  $\text{mA cm}^{-2}$ ,  $I_p^{\text{st}}$  was negligible, probably because the HER rate was too small to fill the subsurface layer before complete surface coverage by zinc.

Figure 8 shows the dependence of  $I_p^{\text{max}}$  and  $I_p^{\text{st}}$  on  $\text{ZnCl}_2$  concentration for a constant electrodeposition current density of 30  $\text{mA cm}^{-2}$ .  $I_p^{\text{max}}$  and  $I_p^{\text{st}}$  decreased sharply when  $\text{ZnCl}_2$  concentration increased up to 0.36 M  $\text{ZnCl}_2$  and reached very low values at a higher  $\text{ZnCl}_2$  concentration. It can be assumed that this stronger barrier effect to hydrogen permeation is due to a higher compactness of the zinc coating. These results are of practical importance. They reveal that intensive hydrogenation of the substrate may occur below a critical  $\text{ZnCl}_2$  concentration (about 0.36 M). These data are in full agreement with the work of Trejo et al. [30] who used a bath containing 0.01, 0.4 or 0.6 M

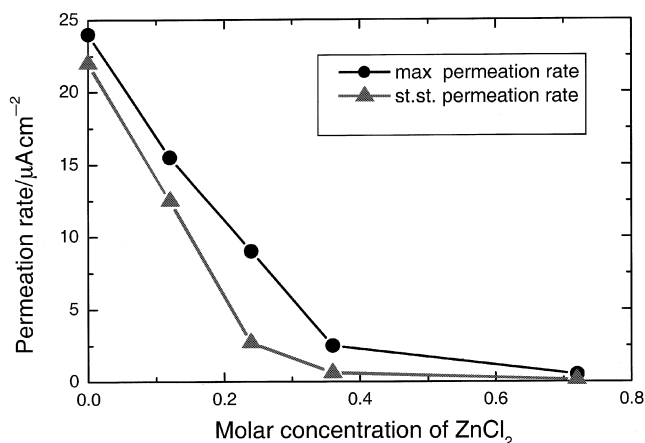


Fig. 8. Maximum permeation rate (●) and steady state permeation rate (▲) against molar concentration of  $\text{ZnCl}_2$  during zinc electrodeposition. (Current density 30  $\text{mA cm}^{-2}$ ).

$\text{ZnCl}_2$  in 2.8 M KCl solution and who observed that dense coatings were obtained with  $\text{ZnCl}_2$  concentration equal to or higher than 0.4 M  $\text{ZnCl}_2$ .

Figure 9 shows voltammograms obtained in a pure plating bath (PB) containing 0.24 M  $\text{ZnCl}_2$  in 2.7 M KCl + 0.24 M  $\text{H}_3\text{BO}_3$  with additives Na-B, PEG, SAA, BA and their combination. The additive BA, as well as the combined additive (all additives), strongly inhibit zinc electrocrystallization, the effect being more intense with the combined additive.

The comparison between the permeation transients obtained at 30  $\text{mA cm}^{-2}$  from PB in the absence and presence of additives (Figure 10) shows that the permeation rate decreases in the following order: Na-B, BA, SAA, PB, PEG, all additives. The additive SAA exerts a negligible effect on hydrogen permeation. Na-B and BA, separately added to the pure electrolyte, enhance hydrogenation of the steel substrate. The large integral area of the transient obtained in the presence of Na-B means that a very high quantity of hydrogen permeates through the zinc coating. This effect is probably a

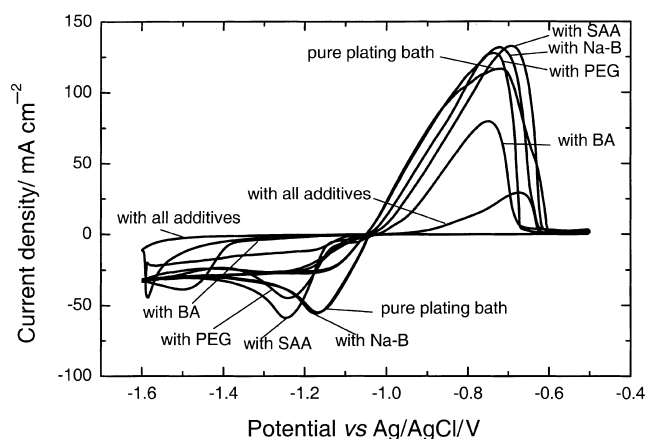


Fig. 9. Polarization curves in the zinc plating bath without or with Na-B, PEG<sub>6000</sub>, SAA and BA additives. (Scan rate 25  $\text{mV cm}^{-1}$ , 0.24 M  $\text{ZnCl}_2$ ).

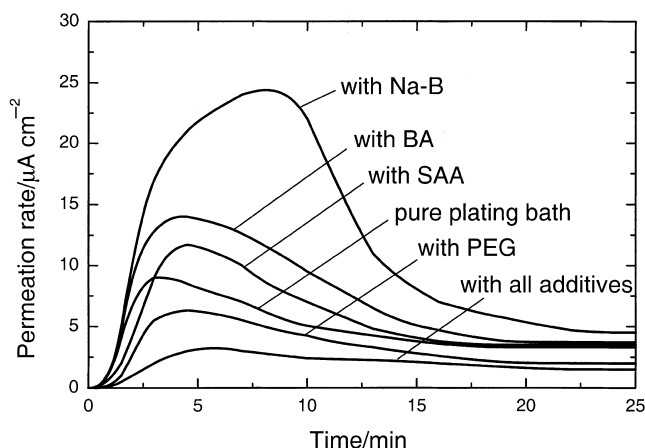


Fig. 10. Hydrogen permeation transients obtained during zinc electro-deposition from a plating bath without or with Na-B, PEG<sub>6000</sub>, SAA and BA additives. (0.24 M ZnCl<sub>2</sub>, current density 30 mA cm<sup>-2</sup>).

consequence of the formation of a porous or dendritic coating. In the presence of Na-B or BA, hydrogenation is enhanced at the beginning of the process (up to 5 min). This phenomenon is dangerous because, according to [12], the critical amount of hydrogen which may cause embrittlement is evolved during electrodeposition of the initial atomic layers of the coating.

In the presence of PEG or of all additives together, the permeation transients can be related to a lower hydrogen coverage and/or a lower coating porosity. These results are in agreement with literature data [31] showing that polyethylene glycols are efficient inhibitors of hydrogenation of steel during zinc plating. The effect of PEG (more evident at higher MW) is attributable to the formation of a dense and strong adsorbed layer on the cathodic surface. Hydrogen absorption is hindered and recombination of hydrogen atoms to form molecular hydrogen is enhanced. In the same way, the inhibitive action of the combination of additives can be attributed to the formation of a strong adsorbed layer, as well as to an increase in overpotential. As a result, the Zn nucleation rate is enhanced, giving rise to more numerous grains which cover the substrate more rapidly. Therefore, the synergetic action of all additives leads to enhanced recombination of hydrogen atoms, as well as to deposition of a more compact zinc coating, as compared with the case when these additives are present separately in the electrolyte.

#### 4. Conclusion

The permeation transients of steel during cathodic polarization in a blank 2.7 M KCl solution show that the permeation rate increases with increasing cathodic current density while permeation efficiency decreases. For high charging current densities, the permeation current exhibits abnormal behaviour due to the blocking effect of molecular hydrogen. Agitation of the solution, or the use of a surfactant, leads to acceleration in the

departure of hydrogen gas from the steel surface and, as a result, to increased hydrogen permeation. Na-B or PEG<sub>6000</sub> additives change the permeation process in the opposite manner as a result of their contrary effects on the recombination of adsorbed hydrogen at the steel surface: the hydrogenation of steel is decreased by a factor of two in the presence of PEG<sub>6000</sub> in KCl solution, whereas it is increased by a factor of two in the presence of Na-B.

The permeation transients obtained in a pure KCl + ZnCl<sub>2</sub> plating bath reveal that there was a critical concentration of ZnCl<sub>2</sub> (about 0.36 M) below which very intensive hydrogenation of the steel substrate occurred.

Hydrogen permeation in the steel substrate is inhibited when PEG<sub>6000</sub> is added to the plating bath, and even more when the combination of four additives is used. This effect can be attributed both to the low hydrogen coverage of the steel and to the low porosity of the coating. The use of such additives is an appropriate method of avoiding the deleterious effects of hydrogen embrittlement due to zinc plating.

#### Acknowledgement

This work was supported by the Bulgarian Academy of Sciences (Bulgaria) and the Centre National de la Recherche Scientifique (France) in the framework of a cooperative research program.

#### References

1. K.J. Vetter, 'Electrochemical Kinetics' (Academic Press, New York, 1967), pp. 525-535.
2. J.O'M. Bockris and D.F.A. Koch, *J. Phys. Chem.* **64** (1961) 1941.
3. R.J. Barton, *Proc. Am. Electroplaters Soc.* **47** (1960) 30.
4. A.N. Frumkin, *Z. Phys. Chem.* **207** (1957) 321.
5. M.A.V. Devanathan and Z. Stachurski, *J. Electrochem. Soc.* **111** (1964) 619.
6. M.H. Abd Elhamid, B.G. Ateya and H.W. Pickering, *J. Electrochem. Soc.* **144** (1997) No4 L58.
7. T. Zakroczymski, *J. Electrochem. Soc.* **145** (1998) 1142.
8. D.M. Drazic, in B.E. Conway, J.O'M. Bockris and R.E. White (Ed.), 'Modern Aspects of Electrochemistry', vol. 19 (Plenum Press, New York, 1989), p. 69.
9. H. Vehoff, in H. Wipf (Ed), 'Topics in Applied Physics', vol. 73 (Springer Verlag, Berlin, 1997), p. 215.
10. M. Smialowski, 'Hydrogen in Steel' (Pergamon, London, 1962).
11. R. Oriani, *Corrosion* **43** (1987) 390.
12. W. Paatsch, *Metalloberfläche* **32** (1978) 546.
13. M. Monev, L. Mirkova, I. Krastev, Hr. Tsvetkova, St. Rashkov and W. Richterling, *J. Appl. Electrochem.* **28** (1998) 1107.
14. T. Casanova, F. Soto, M. Eyraud and J. Crousier, *Corrosion Sci.* **39** (1997) 529.
15. M.A.V. Devanathan and Z. Stachurski, *Proc. Roy. Soc. (Lond.)* **A270** (1962) 90.
16. M.A.V. Devanathan, Z. Stachurski and W. Beck, *J. Electrochem. Soc.* **110** (1963) 886.
17. I.A. Bagotskaya, *Zh. Fiz. Khim.* (in Russian) **36** (1962) 2667.
18. J.O'M. Bockris, J. McBreen and L. Nanis, *J. Electrochem. Soc.* **112** (1965) 1025.
19. W. Beck, J.O'M. Bockris, J. McBreen and L. Nanis, *Proc. Roy. Soc. (Lond.)* **A290** (1966) 220.

20. E. Gileadi, M.A. Fullenwider and J.O'M. Bockris, *J. Electrochem. Soc.* **113** (1966) 926.
21. S. Wach, *Brit. Corr. J.* **6** (May 1971) 114.
22. S. Wach, A.P. Miodownik and J. Mackowiak, *Corr. Sci.* **6** (1966) 271.
23. Z. Amrani, F. Huet, M. Jérôme, P. Manolatos and F. Wenger, *J. Electrochem. Soc.* **141** (1994) 2059.
24. A. Knödler, *Metalloberfläche* **40** (1986) 515.
25. S. Venkatesan, R. Subramanian and M.A.V. Devanathan, *Metal Finish.* (May 1966) 50.
26. Th.C. Franklin, *Plat. Surf. Finish.* **4** (1994) 62.
27. 'Combined additive in medium acidic chloride electrolyte for zinc electroplating', *Bulg. Patent 54483* (1981).
28. W. Raczynski and S. Talbot-Besnard, *C.R. Acad. Sci. (France)* **269** (1969), series, 294–296, 1253–1256 and 1498–1501.
29. J. McBreen, L. Nanis and W. Beck, *J. Electrochem. Soc.* **113** (1966) 1218.
30. G. Trejo, R.B. Ortega, Y.V. Meas, P.E. Ozil, E. Chainet and B. Nguyen, *J. Electrochem. Soc.* **145** (1998) 4090.
31. C.M. Beloglazov 'Hydrogenation of Steel During Electrochemical Processes' (Leningrad University Press, Leningrad, 1975), p. 324 (in Russian).